

UC Berkeley

Research Reports

Title

Identifying Density-Flow Relations on Arterial Surface Streets

Permalink

<https://escholarship.org/uc/item/8685r9ks>

Authors

Ahn, Soyoung
Cassidy, Michael J.

Publication Date

2002-08-19

CALIFORNIA PATH PROGRAM
INSTITUTE OF TRANSPORTATION STUDIES
UNIVERSITY OF CALIFORNIA, BERKELEY

Identifying Density-Flow Relations on Arterial Surface Streets

Soyoung Ahn
Michael J. Cassidy
University of California, Berkeley

California PATH Research Report
UCB-ITS-PRR-2002-26

This work was performed as part of the California PATH Program of the University of California, in cooperation with the State of California Business, Transportation, and Housing Agency, Department of Transportation; and the United States Department of Transportation, Federal Highway Administration.

The contents of this report reflect the views of the authors who are responsible for the facts and the accuracy of the data presented herein. The contents do not necessarily reflect the official views or policies of the State of California. This report does not constitute a standard, specification, or regulation.

Final Report for TO 4109

August 2002

ISSN 1055-1425

Identifying Density-Flow Relations on Arterial Surface Streets

By Soyoung Ahn and Michael J. Cassidy

University of California
Department of Civil and Environmental Engineering
and the Institute of Transportation Studies
416 McLaughlin Hall
Berkeley, CA 94720
(510)642-7702
cassidy@ce.berkeley.edu

August 19, 2002

Abstract

A simple car-following rule was verified by studying vehicles discharging from long queues at signalized intersections. These observations indicated that the time-space trajectory of a j^{th} vehicle discharging on a homogeneous intersection approach was essentially the same as the $j-1^{\text{th}}$ vehicle except for a translation in space and time. This is in agreement with a simplified theory proposed by G.F. Newell. The finding indicates that the congested branch of a density-flow curve is linear in form.

1. Introduction

The literature on car-following theories is extensive. One of the earliest and perhaps best known of these models was proposed by Chandler, et.al. (1958). According to this model, a driver accelerates (or decelerates) in response to the velocity changes of the vehicle immediately downstream. Each such acceleration of the driver occurs following a time lag. Much of the work related to this theory was concerned with how the values of the time lag affect stability; i.e., early research sought to identify whether the car-following process is marked by disturbances that amplify or decay as they propagate through traffic.

In later work by Kometani and Sasaki (1961), a model was proposed whereby a driver chooses a velocity as a function of her spacing. The time lag preceding the driver's changes in velocity was interpreted as a reaction time.

The present study supports a car-following theory proposed by Newell (2002) that is less elaborate than its predecessors in that it uses fewer parameters as well as a different logic. According to this simple theory, a driver selects her preferred spacings for given velocities in such way(s) that a vehicle's trajectory looks like that of its leader, but with a translation in time and space. Disturbances therefore neither amplify nor decay. Rather, they propagate as waves through traffic at an average speed independent of the vehicle velocity. This means the congested branch of the density-flow curve is linear in form.

The logic behind Newell's simplified model is described more completely in the following section. Our methods of extracting and analyzing traffic data followed directly from this logic, as described in section 3. Namely, we recorded on video the motions of queued vehicles as they discharged into signalized intersections during initial periods of the green. From these videos, we measured vehicle trajectories. The temporal and spatial translations between consecutive trajectories were found to come from a common joint probability distribution, just as described in Newell's theory. The statistical tests used for this verification, along with the outcomes of these tests, are described in section 4. Certain implications of our findings are noted in the conclusions. Some limitations of Newell's theory and areas of future work are discussed there as well.

2. Background

The vehicle trajectories in Fig. 1(a) are used to explain Newell's very simple car-following model and to clarify its differences from other theories on the subject. The $j-1^{\text{th}}$ vehicle shown here initially travels at a constant velocity, v . Newell conjectures that vehicle j will follow at the same velocity, assuming v is less than j 's desired velocity, V_j . In this way, driver j maintains her desired spacing with $j-1$. Since vehicles are traveling on a homogeneous road segment, this spacing will remain the same so long as the velocity of $j-1$ is unchanged.

If, however, $j-1$ alters its velocity, say from v to v' , and then remains at this new velocity v' for some time, its actual trajectory can be approximated by piece-wise linear extrapolations. (Such extrapolations are used for the trajectories in Fig. 1(a)). If $v' < V_j$, vehicle j will, according to the model, change velocity in a manner like that of $j-1$. The

point marking j 's velocity change is displaced from that of its leader by a distance d_j and a time τ_j , as shown in the figure. In short, if a $j-1^{\text{th}}$ vehicle maintains a new speed (e.g. v') for a sufficient duration, the j^{th} vehicle changes its velocity upon reaching the spacing that driver j chooses for the new velocity (v'). This spacing is designated s_j' in Fig. 1(a) and the time required for j to reach this spacing is τ_j . The τ_j and the d_j are assumed to be independent of j 's velocity. Moreover, these translations are assumed to vary with each j^{th} driver as if they were sampled independently from a joint probability distribution.

The wave connecting the changes from one (piece-wise linear) trajectory to the next therefore propagates as a random walk. The mean wave speed is d/τ , where d is the arithmetic average of the spatial translations taken across drivers and τ is the analogous average of the temporal translations.

The model can be iterated over many vehicles, such that the location of any j^{th} vehicle at some time is a suitable translation of a (perhaps arbitrary) lead vehicle. The leader may be separated from j by many vehicles.

The reader should appreciate that τ_j is not a reaction time. (As noted above, it is instead the time needed for driver j to reach her preferred spacing for a new velocity). Newell's model is thus based upon drivers' preferred following distances for given velocities in a way that distinguishes it from most other car-following theories. It follows that each driver adopts her own relation between velocity and spacing and, as shown in Fig. 1(b), this relation is linear with slope τ_j .¹

Finally, Newell transformed his car-following model into a macroscopic one for describing average driver behavior. In this way, he established a connection between his theory and fluid models. This simple transformation leads to a linear relation between queued flows and densities, as shown in Fig. 1(c).² This form indicates that in queued traffic, flow is a linear decreasing function of density and the relation depends upon d and τ . The average wave speed, d/τ , is independent of vehicle velocities.

The previous paragraph is particularly relevant to PATH project T.O. 4109. The objective of this work has been to identify the shape of the congested branch of density-

¹ That the slope of each j 's spacing-speed relation is τ_j follows from the trajectories in Fig. 1(a) showing that j 's spacing, s_j , equals $d_j + v \cdot \tau_j$.

² That the macroscopic relation between queued densities and flows is linear follows from the previous discussion, but the reader can refer to *Newell (2002)* for the simple analytical derivation.

flow curves for arterial surface streets. By verifying Newell's simple car-following model, we have shown that this branch of the curve is linear in form.

3. Data and Study Scope

The methods used in this study to verify Newell's car-following theory followed from the logic just described. We measured the trajectories of vehicles as they discharged from long queues on homogeneous approaches to signalized intersections. Some of the temporal and spatial translations that marked velocity changes across trajectories were very evident, thanks to waves that arose in the queues. These observed translations were found to have come from a common joint distribution, as per Newell's simple theory.

The data were obtained by video-taping traffic on the arterial approaches to two signalized intersections, both located in Oakland, California. These are illustrated in Figs. 2(a) and (b). This data collection took place during afternoon rush periods in 2001 and videos were taken of multiple travel lanes at each of the two intersections, as annotated in the figures. The queues in each of these lanes grew to include 10 vehicles or more in virtually every cycle captured in our videos. To record these long queues in their entirety, the videos were taken from top floors of tall buildings nearby.

The trajectories for many of these discharging vehicles were constructed by measuring (from video) the times each passed fixed reference points along the intersection approaches. These reference points were separated by short distances of 3 to 6 m (10 to 20 ft) and each vehicle's passage times were plotted in the time-space plane. A polynomial trend line was then fit to each set of such points corresponding to a unique vehicle. The order of a polynomial curve was determined on a case by case basis, depending upon the pattern of measured points that mapped the vehicle's motion.

Each trajectory was then approximated using piece-wise linear interpolations to its smooth polynomial curve, as illustrated in Fig. 3. These interpolations were drawn through the points corresponding to vehicle velocities just above 0 km/h, 6.5 km/h, 13 km/h, and 19.5 km/h (0 mph, 4 mph, 8 mph and 12 mph), as shown in the figure. (The reader will note the slopes of a polynomial curve are the instantaneous velocities estimated for that vehicle). The waves emanating from the changes in these piece-wise

linear trajectories are shown in Fig.3 as heavy dashed lines and the slope of any such line is the wave's speed.

Notably, these trajectories were not constructed for all the discharging vehicles observed on video. Thus, measurements were not usually taken of each trajectory's temporal and spatial translations along wave paths. Instead, most of the observations were collected in a more aggregate fashion, as described below. This greatly simplified the task of data extraction and it provided for an effective way of validating Newell's model.

For each lane, and for each signal cycle, trajectories were constructed for the first several vehicles in queue as they discharged into the intersection. In some cases, it was clear that the first one or two of these vehicles accelerated faster than the vehicle directly behind. Since the latter did not keep up with the vehicle(s) ahead, it was taken as the leader of the discharging queue. The trajectory of the last vehicle in queue was also constructed.

For each cycle m , the number of queued vehicles in a given lane, n_m , was noted. We then measured the $T(n_m)$ and $D(n_m)$, the total time and distance covered by a wave propagating through a queue, as illustrated in Fig. 3. These $T(n_m)$ and $D(n_m)$ were separately measured for each of the four waves described by the piece-wise linear trajectories.

According to Newell's theory, the $[T(n_m), D(n_m)]$ is a bivariate process with independent increments. This assumption of independence was verified by measuring the τ_j and d_j for various vehicle j after we constructed the piece-wise linear trajectories for each and every vehicle discharging from a sample of the queues captured in our videos.

Thus, the $[T(n_m), D(n_m)]$ can be described by a bivariate normal distribution with mean and covariance matrix proportional to n_m , i.e.,

$$[T(n_m), D(n_m)] \sim BVN \left([\tau \times n_m, d \times n_m]; \begin{bmatrix} \sigma_\tau^2 & \sigma_{d\tau} \\ \sigma_{\tau d} & \sigma_d^2 \end{bmatrix} \times n_m \right) \quad \text{Equation 1}$$

Since the n_m varied with m , samples taken in each cycle were not identically distributed. The five parameters in Equation 1 (τ , d , σ_τ^2 , σ_d^2 and $\sigma_{\tau d}$) were therefore obtained using maximum likelihood estimation (*Stone, 1996*). These parameters were separately estimated for each of the four wave types in a given lane. They were then estimated again from the $[T(n_m), D(n_m)]$ measured for all (four) waves in a lane.

These estimates were next used in a likelihood ratio test (*Stone, 1996*). The outcome indicated that the same bivariate normal distribution can be used for describing $[T(n_m), D(n_m)]$ for any of the four waves in a given lane. The test thus confirmed Newell's hypothesis that $[\tau_j, d_j]$ vary as if they were sampled independently from some joint probability distribution.

It is notable that our validation methods used trajectories that were, in reality, continually accelerating; i.e., most vehicles videoed in the discharging queues did not actually maintain a fixed velocity for an extended period. That our tests nonetheless support Newell's theory attests to the robust nature of his simple model. These tests will now be described in the following section.

4. Verifying the Theory

The presentations in this section show that the $[\tau_j, d_j]$ in each lane came from a common joint distribution. To this end, we first verified the assumption underlying Equation 1; i.e., that the $[T(n_m), D(n_m)]$ has independent increments. This was done by constructing the piece-wise linear trajectories for all of the discharging vehicles from a sample of the queues. The temporal and spatial translations between consecutive trajectories were then measured along the waves.

Some typical examples of these samples are presented as lag-one scatter-plots in Figs. 4(a)-(d). The samples in each plot were taken from a single lane for one of the four different wave types; this information is labeled in the figure. Each plot displays the measured spatial or temporal translation for a j^{th} vehicle vs that translation observed for its neighbor $j+1$. In every case, the pattern of data scatter reveals no trends or correlations. The $[\tau_j, d_j]$ can therefore be taken as independent across drivers.

Maximum likelihood estimation was next used to obtain the parameters in Equation 1. Table 1 displays the τ and d estimated in this way. These are provided for

each of the four wave types in each of the observed travel lanes. Also listed in Table 1 are the sample sizes for each estimate, $\sum_{m=1}^M n_m$; where M is the number of cycles observed.

These sample sizes were sufficiently large such that the coefficients of variation for all estimates of τ and d never exceeded 0.10.

Wave Type	McArthur Site						Harrison Site					
	Center Lane			Curb Lane			Median Lane			Center Lane		
	$\sum_{m=1}^M n_m$	τ (sec)	d (m)	$\sum_{m=1}^M n_m$	τ (sec)	d (m)	$\sum_{m=1}^M n_m$	τ (sec)	d (m)	$\sum_{m=1}^M n_m$	τ (sec)	d (m)
v*-> 0	57	1.13	7.12	37	1.54	7.10	84	1.55	9.30	103	1.53	9.06
v = 6.5 km/h	48	1.06	6.79	30	1.40	7.02	80	1.59	9.56	111	1.60	9.24
v = 13 km/h	48	1.18	6.64	37	1.42	7.10	75	1.65	9.39	120	1.61	8.80
v = 19.5 km/h	41	1.35	6.06	27	1.51	6.69	64	1.74	8.82	100	1.61	8.53

Table 1
Means estimated with maximum likelihood and sample sizes
(* v represents velocity displayed by a piece-wise linear trajectory)

Finally, the likelihood ratio test was used to verify that the $[T(n_m), D(n_m)]$ measured for all waves came from the same bivariate normal distribution. This entailed comparing two probability distributions. The first was a general model obtained using the parameters that were separately estimated for each of the four wave types evident from our piece-wise linear trajectories; i.e.

$$\ell^{gen} = \sum_k \sum_m \log \left[BVN \left([\tau_k \times n_{m,k}, d_k \times n_{m,k}], \begin{bmatrix} \sigma_{\tau,k}^2 & \sigma_{d\tau,k} \\ \sigma_{\tau d,k} & \sigma_{d,k}^2 \end{bmatrix} \times n_{m,k} \right) \right], \quad \text{Equation 2}$$

where ℓ^{gen} is the general log likelihood and the subscript k denotes wave type (of which there were four).

The second was a restricted model whereby all observations were combined for estimating the mean and covariance matrix terms; i.e.,

$$\ell^{res} = \sum_k \sum_m \log \left[BVN \left(\left[\tau \times n_{m,k}, d \times n_{m,k} \right]; \begin{bmatrix} \sigma_\tau^2 & \sigma_{d\tau} \\ \sigma_{\tau d} & \sigma_d^2 \end{bmatrix} \times n_{m,k} \right) \right], \quad \text{Equation 3}$$

where ℓ^{res} is the restricted log likelihood.

The log likelihood ratio, $2 \times (\ell^{gen} - \ell^{res})$, has a Chi-Square distribution, in this case with degree of freedom 15; (15 is the number of parameters lost in the restricted model). The log likelihood ratios obtained for each travel lane are shown in Fig. 5. In each instance, these are smaller than 25, the Chi-Square critical value at the 0.05 significance level.

The general and restricted models are therefore identical in a statistical sense; i.e., their differences are insignificant. This means that the same bivariate normal distribution can be used to describe the $[T(n_m), D(n_m)]$ for each of our four wave types; i.e., the distribution is independent of vehicle velocity. It follows that each j^{th} driver's $[\tau_j, d_j]$ came from some common joint probability distribution, as per Newell's simple theory.

5. Conclusions

As platoons accelerate on homogeneous highways, a j^{th} vehicle evidently follows the same trajectory as the $j-1^{\text{th}}$ vehicle except for a translation in time and space. For the data observed in the present work, the translations $[\tau_j, d_j]$ varied as if drawn independently from a joint distribution. The finding supports Newell's simplified car-following theory. This, in turn, is consistent with the macroscopic traffic theory of Lighthill and Whitham (1955) with a triangular shaped density-flow curve.

Our finding does indicate that the congested branch of the density-flow curve is linear in form, at least for the low vehicle velocities observed here. Wave speed was thus the same for different values of flow or density within the ranges observed. In contrast to what is described by non-linear density-flow curves, we observed that accelerating vehicles did not create waves that fanned outward.

It is notable that the effects created by non-linear density-flow curves were not even observed at vehicle velocities very close to zero. We cannot verify, however, that non-linear effects do not arise in queued traffic when vehicle velocities approach desired velocities. These conditions were outside the range of what was studied here since many vehicles in the discharging queues did not reach such high velocities while on the homogeneous approaches to the intersections.

As an aside, non-linear effects apparently do arise in uncongested traffic when flows become high. A recent study of freeway traffic showed that the uncongested branches of occupancy-flow curves were not strictly linear in form (*Cassidy and Anani, 2002*).³ Rather, vehicle velocities dropped slightly below desired velocities as uncongested flows approached freeway capacities. So under these conditions, waves propagate forward at speeds slower than those of the vehicles.

Of further note, Newell's theory is particularly susceptible to vehicle lane-changing maneuvers (i.e., over-taking), as these interrupt car following. Lane changing did not arise in the present study (and indeed these maneuvers are illegal near intersections). But Mauch and Cassidy (*2002*) demonstrate that Newell's theory fails for the case of queued freeway traffic when heavy lane-changing takes place. It would seem that improvements in traffic flow theories will come by incorporating lane-changing effects.

Improved traffic theories should also result by better understanding the influences of geometric inhomogeneities on driver behavior. Of course, Newell's simplified theory is not expected to hold at inhomogeneities and we have even observed an instance of this. In addition to the measurements already described in this manuscript, we examined discharging queues in the curb lane for northbound traffic at the Harrison intersection; see Fig. 2(b). As shown in the figure, the lane has a noticeable inhomogeneity. Namely, its width reduces upstream of the intersection. Not surprisingly, our analyses of the data from this lane indicated that car-following did not occur there as per Newell's theory.

Trajectories in this curb lane are currently being studied to obtain insights into car-following behavior at the inhomogeneity. One cannot model driver behavior at inhomogeneities without first understanding what actually occurs.

³ Occupancy is a dimensionless measure of density.

Finally, the present work did not explicitly verify that a j^{th} driver tends to maintain the same $[\tau_j, d_j]$ over her trip,⁴ even though this driver attribute is also part of Newell's theory. But findings reported from earlier research can now be used as confirmation that this attribute actually occurs.

Previous work by Cassidy and Windover (1998), for example, has shown that individual drivers have their own "personalities" (i.e., different drivers choose different spacings for a given velocity) and that drivers tend to remember their personalities. In light of the present findings reported here, this earlier finding can be taken as support for Newell's contention that a $[\tau_j, d_j]$ is maintained by each driver j .

References

Cassidy, M.J., Anani, S.B. (2002) Stationary models of unqueued freeway traffic and some effects of freeway geometry. *Submitted for journal publication*.

Cassidy, M.J., Windover, J.R. (1998) Driver memory: motorist selection and retention of individualized headways in highway traffic. *Transpn Res.32A*, 129-137.

Chandler, R.E., Herman, R., Montroll, E.W. (1958) Traffic dynamics: studies in car following. *Oper. Res.* 6, 165-184.

Kometani, E., Sasaki, T. (1961) Dynamic behavior of traffic with a nonlinear spacing. In: Herman, R. (Ed.), *Theory of Traffic Flow*. Elsevier, Amsterdam, pp. 105-119.

Lighthill, M.J., Whitham, G.B. (1955) On kinematic waves in highway traffic. I Flood movement in long rivers. II A theory of traffic flow on long crowded roads. *Proc. Roy. Soc. (London) A229*, 281-345.

Mauch, M., Cassidy, M.J. (2002) Freeway traffic oscillations: observations and predictions. *In press*: Taylor, M.A.P. (Ed.), *Traffic and Transportation Theory*, Elsevier, Amsterdam.

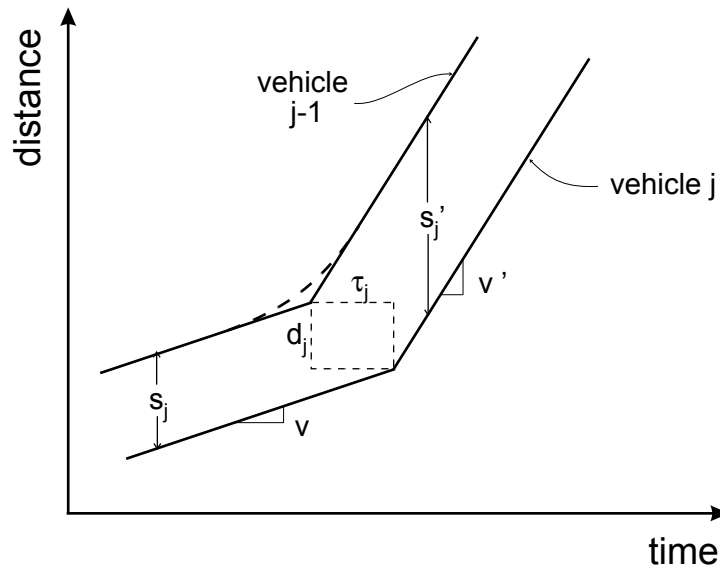
Newell, G.F. (2002) A simplified car-following theory: a lower order model. *Transpn Res.* 36B, 195-205.

Stone, C.J. (1996) *A course in probability and statistics*, Belmont: Duxbury Press

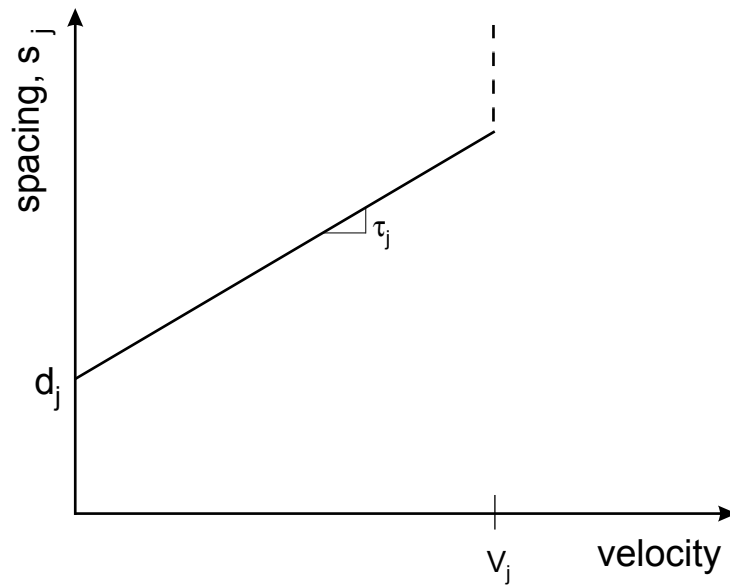
⁴ Each j^{th} piece-wise linear trajectory revealed only four waves and therefore yielded only four joint observations of $[\tau_j, d_j]$. This would be too small a sample from which to draw conclusions. Additional observations could have been obtained for each j by constructing the piece-wise linear trajectories with more incremental changes in velocity. However, this would have brought higher estimation errors.

List of Figures

- Figure 1. (a) Piece-wise linear vehicle trajectories (adopted from Newell, 2002)
(b) Relation between velocity and spacing for an individual driver
(adopted from Newell, 2002)
(c) Density-flow curve for Newell's theory
- Figure 2. (a) McArthur site
(b) Harrison site
- Figure 3. Construction of piece-wise trajectories and the waves they reveal.
- Figure 4. (a) τ_j vs τ_{j+1} ; curb lane of McArthur site; wave marking vehicle velocity of 6.5 km/h
(b) d_j vs d_{j+1} ; curb lane of McArthur site; wave marking vehicle velocity of 6.5 km/h
(c) τ_j vs τ_{j+1} ; median lane of Harrison site; wave marking vehicle velocity of 13 km/h
(d) d_j vs d_{j+1} ; median lane of Harrison site; wave marking vehicle velocity of 13 km/h
- Figure 5. Results of ratio tests showing $[T(n_m), D(n_m)]$ is independent of vehicle velocity



(a)



(b)

Figure 1

- (a) Piece-wise linear vehicle trajectories (adopted from Newell, 2002)
- (b) Relation between velocity and spacing for an individual driver (adopted from Newell, 2002)

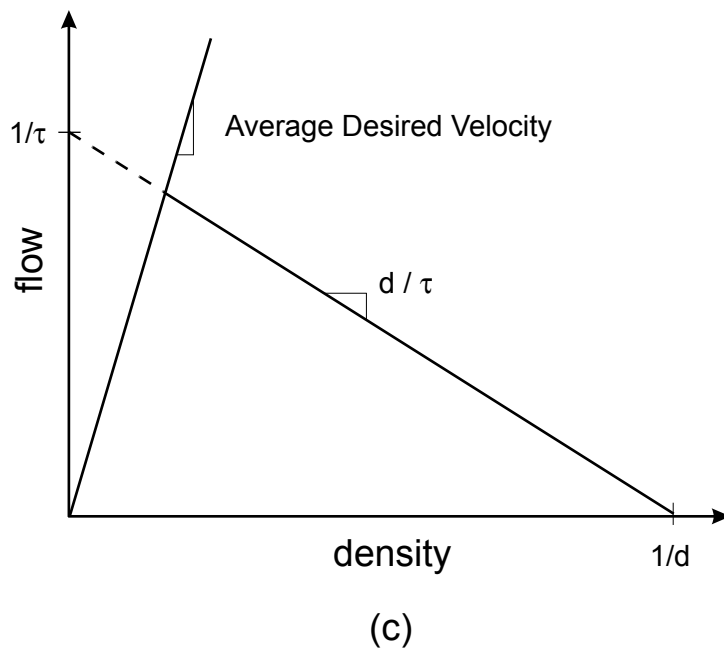
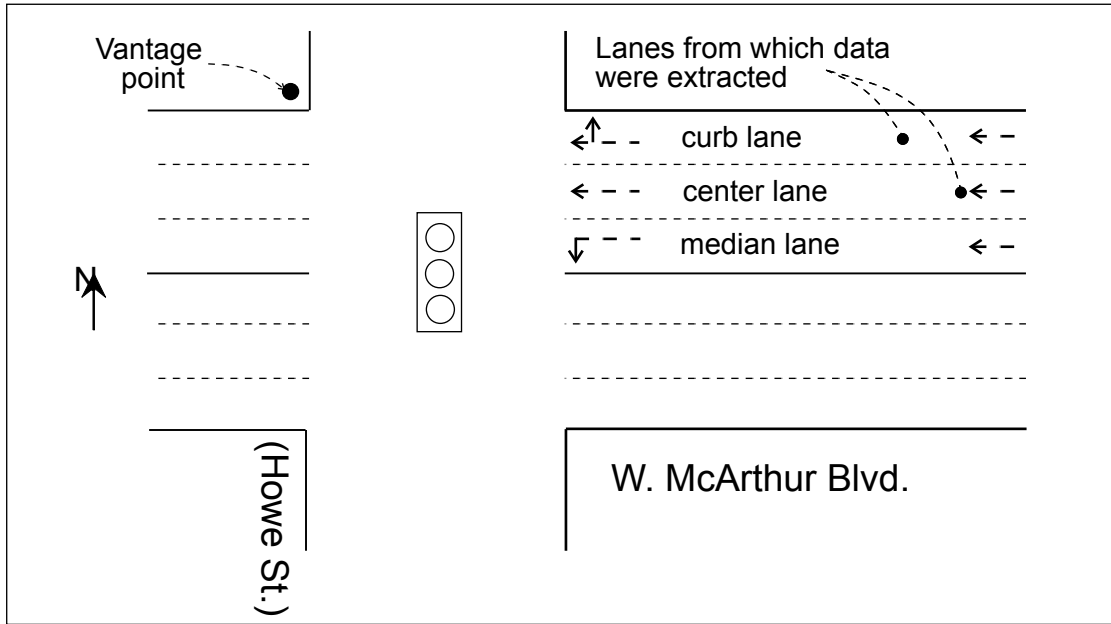
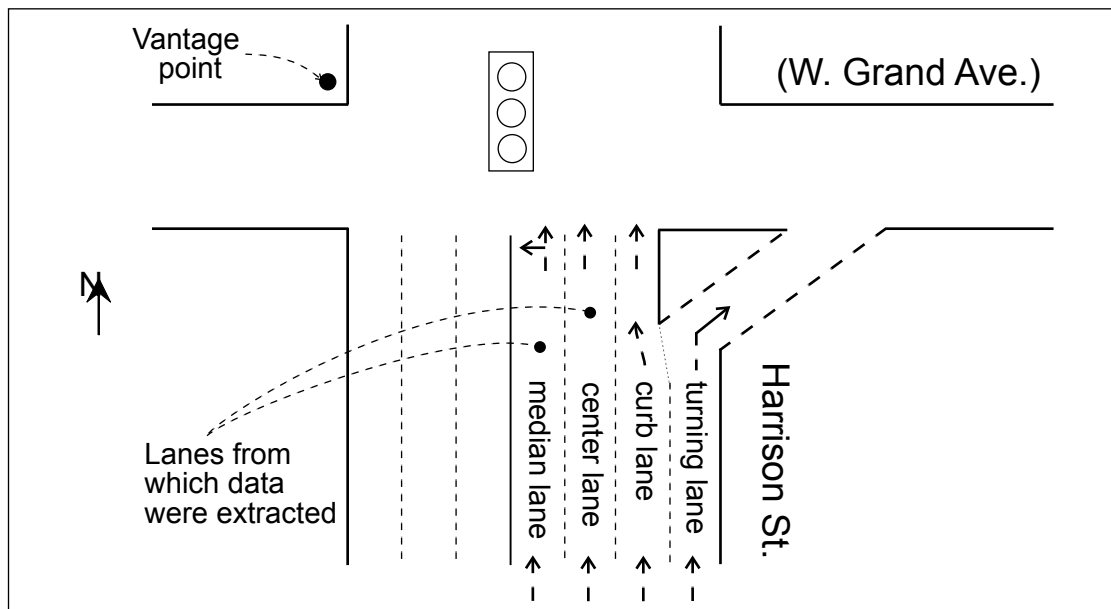


Figure 1 (con't)

(c) Density-flow curve for Newell's theory



(a)



(b)

Figure 2
 (a) McArthur site (b) Harrison site

(Note: Left turns from the northbound approach at the Harrison site are performed on a protected basis, i.e., without conflicts from the opposing direction.)

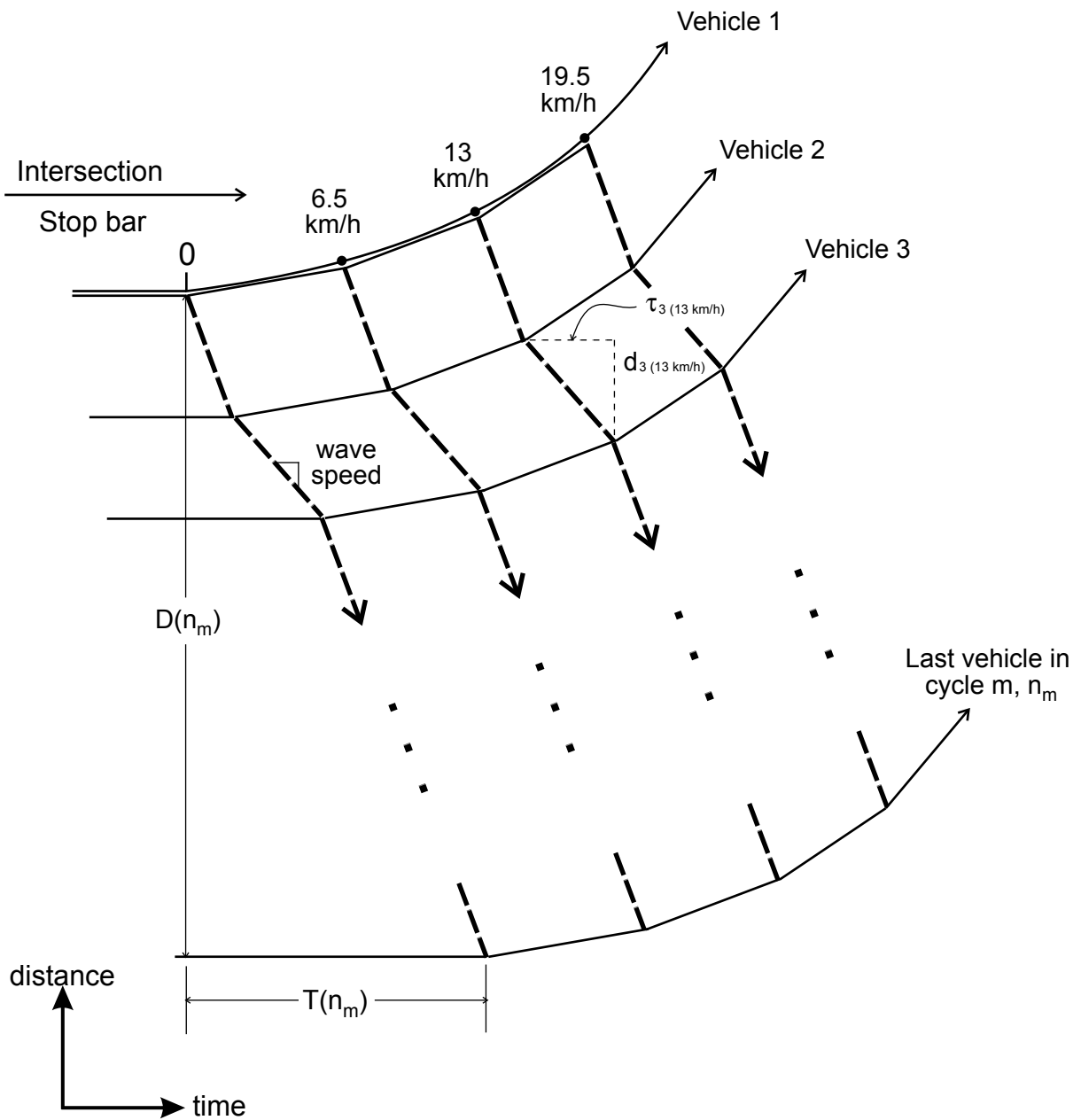


Figure 3

Construction of piece-wise trajectories and the waves they reveal.
 (Note: Waves are displayed as heavy dashed lines.)

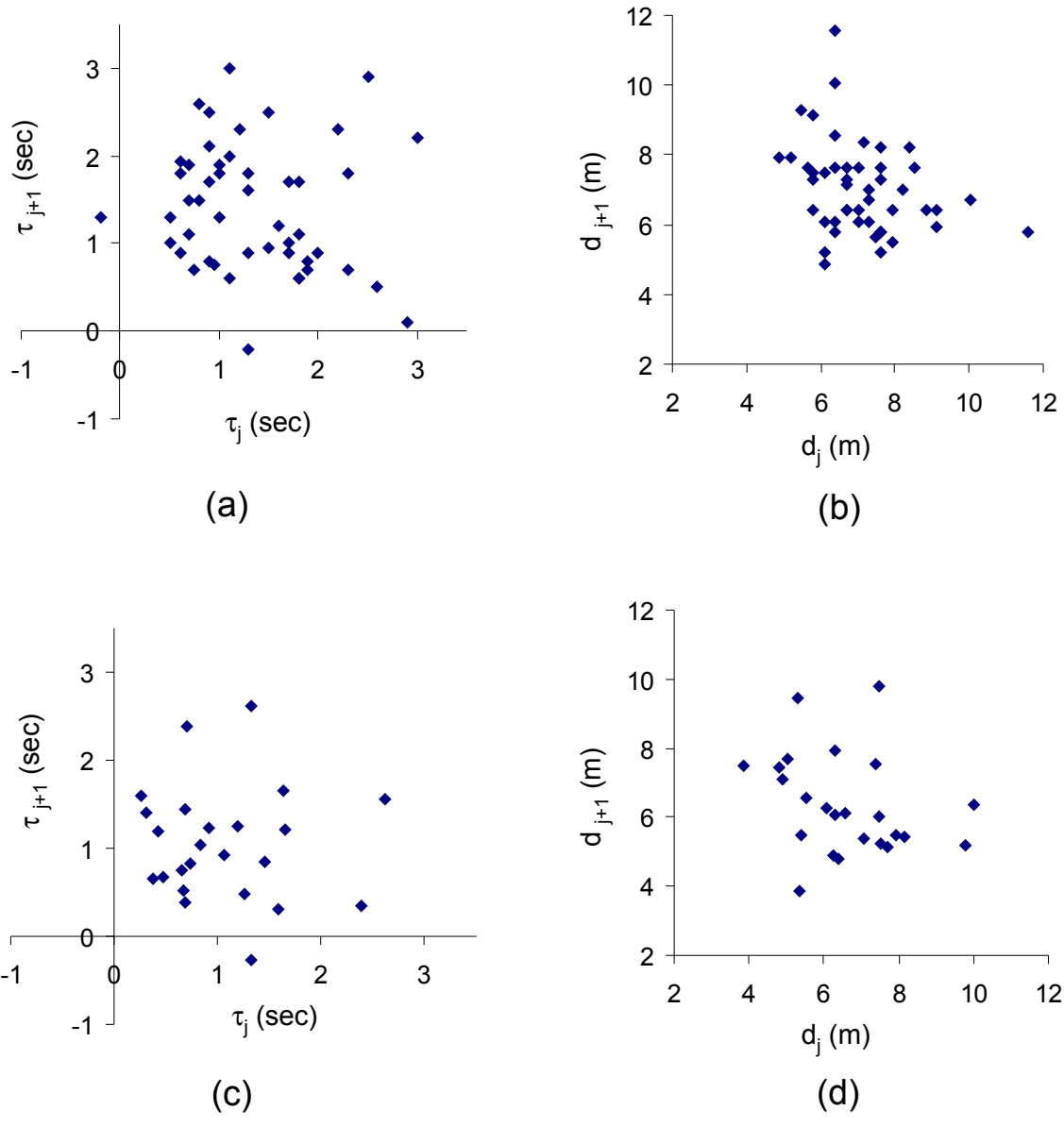


Figure 4. Lag-one scatter-plots

- (a) τ_j vs τ_{j+1} ; curblane of McArthur site;
wave marking vehicle velocity of 6.5 km/h
- (b) d_j vs d_{j+1} ; curblane of McArthur site;
wave marking vehicle velocity of 6.5 km/h
- (c) τ_j vs τ_{j+1} ; median lane of Harrison site;
wave marking vehicle velocity of 13 km/h
- (d) d_j vs d_{j+1} ; median lane of Harrison site;
wave marking vehicle velocity of 13 km/h

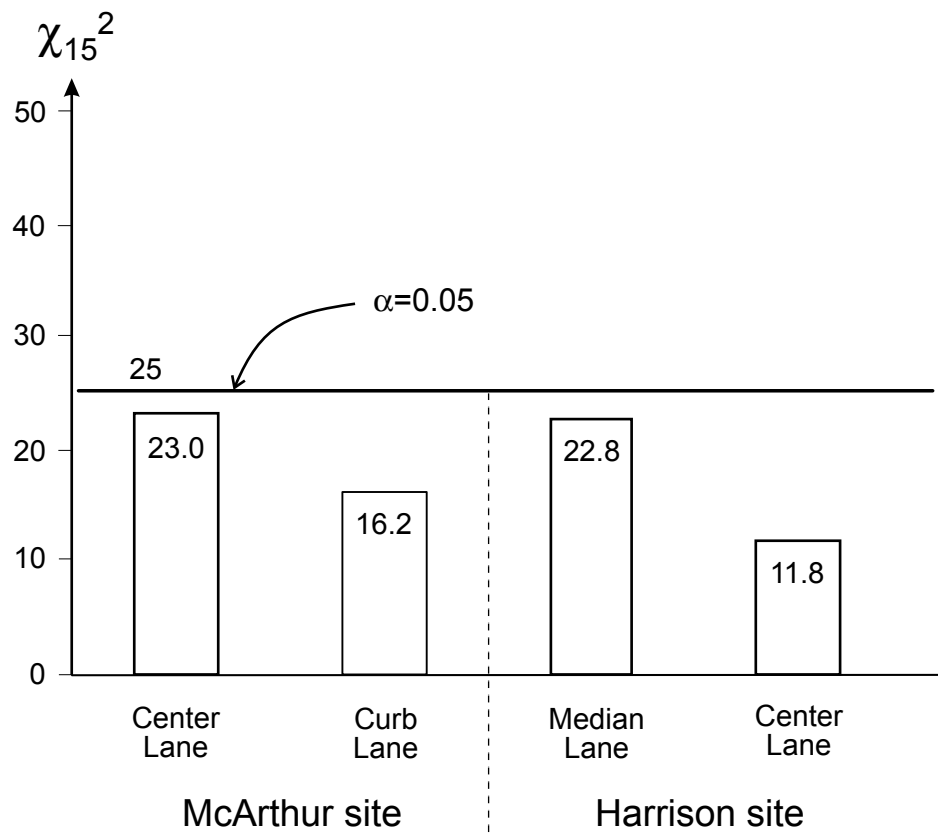


Figure 5
 Results of ratio tests showing $[T(n_m), D(n_m)]$ is independent of vehicle velocity